Understanding the interfacial behavior of lysozyme on Au (111) surfaces with multiscale simulations

Mohammadreza Samieegohar, Heng Ma, Feng Sha, Md Symon Jahan Sajib, G. Iván Guerrero-García, and Tao Wei

Citation: Appl. Phys. Lett. **110**, 073703 (2017); doi: 10.1063/1.4976516
View online: http://dx.doi.org/10.1063/1.4976516
View Table of Contents: http://aip.scitation.org/toc/apl/110/7
Published by the American Institute of Physics

Understanding the interfacial behavior of lysozyme on Au (111) surfaces with multiscale simulations

Mohammadreza Samieegohar,[1] Heng Ma,[1] Feng Sha,[2] Md Symon Jahan Sajib,[1] G. Iván Guerrero-García,[3] and Tao Wei[1]
[1]*Dan F. Smith Department of Chemical Engineering, Lamar University, Beaumont, Texas 77710, USA*
[2]*Network Information Center, Xiamen University of Technology, Xiamen 361024, China*
[3]*CONACYT-Instituto de Física, Universidad Autónoma de San Luis Potosí, San Luis Potosí 78000, Mexico*

(Received 22 November 2016; accepted 1 February 2017; published online 15 February 2017)

The understanding of the adsorption and interfacial behavior of proteins is crucial to the development of novel biosensors and biomaterials. By using bottom-up atomistic multiscale simulations, we study here the adsorption of lysozyme on Au(111) surfaces in an aqueous environment. Atomistic simulations are used to calculate the inhomogeneous polarization of the gold surface, which is induced by the protein adsorption, and by the presence of an interfacial layer of water molecules and monovalent salts. The corresponding potential of mean force between the protein and the gold surface including polarization effects is used in Langevin Dynamics simulations to study the time dependent behavior of proteins at finite concentration. These simulations display a rapid adsorption and formation of a first-layer of proteins at the interface. Proteins are initially adsorbed directly on the gold surface due to the strong protein-surface attractive interaction. A subsequent interfacial weak aggregation of proteins leading to multilayer build-up is also observed at long times. *Published by AIP Publishing*. [http://dx.doi.org/10.1063/1.4976516]

Fundamental studies of interfacial phenomena between biomolecules and substrate surfaces are critical to the development of novel biotechnologies[1,2] and anti-biofouling (or anti-biocorrosion) materials, such as peptoids[3] and zwitterionic polymers.[4] Protein adsorption is also related to biological processes such as cell or bacterial attachment,[5] and can induce interfacial electron transfer[6] or surface polarization[7,8] in metallic interfaces. Billions of dollars are spent annually to control marine biofouling by governments and industries.[5] Interfacial phenomena are also commonly found in various experimental bio-sensing techniques, such as Fourier Transform Infrared Spectroscopy/Attenuated Total Reflectance (FTIR/ATR)[9] and Surface Plasmon Resonance (SPR).[10] The recently developed label-free and restriction-free technique of Transient Induced Molecular Electronic Spectroscopy (TIMES)[2] can measure protein-ligand binding under relevant physiological conditions of the bulk solution inside a microfluidic channel by detecting the induced polarization response on metallic electrode's surfaces upon mass transfer of biomolecules. It is very important to understand the bio-interfacial phenomena in order to interpret experimental signals.

Over the last two decades, a plethora of experimental and simulation studies have shown that protein adsorption behavior on surfaces can be affected by many factors, such as surface tension,[11] surface charge distribution,[12] morphology,[13,14] roughness,[15] wettability,[16] buffer's ions,[9] and protein surface's heterogeneity[17] in charge and hydrophobicity. Our previous atomistic simulations[6,11] showed that for neutral surfaces, the surface tension of substrate surfaces serves as a dominant driving force in the protein adsorption, whereas the protein dehydration is the main barrier force preventing adsorption. On the other hand, electrostatic surface polarization induced by small molecules has been extensively investigated through quantum computation[18] and hybrid quantum mechanics and molecular mechanics (QM/MM).[19] In addition, efficient empirical molecular dynamics simulations[7,8,20] with polarizable surface force field parameters have recently been developed for surfaces made of gold,[7] silver,[8] and graphite[20] by introducing dummy atoms to form rigid-rod dipoles. Those dipoles are free to rotate around atomic sites of the gold lattice to mimic dynamic dipole responses of the surface upon the adsorption of peptides or proteins. Such studies have shown that the contribution of the electrostatic surface polarization can account for about 10%–20% of the total protein binding energy,[21,22] although the energy due to polarization is less than 10% of the water-metal surface binding energy.[22]

Different protein adsorption kinetic models[23] (Langmuir, random sequential adsorption,[24] multiple-states,[25–27] monomer/dimmer exchange,[28] displacement, rollover,[26] surface clusters,[29] and tracking model[30]) take into account various effects such as size repulsion,[23] jamming-limit packing,[23] structural rearrangement,[23,25,27] bulk aggregation,[28] reorientation,[26] lateral interactions,[28–30] and cooperative adsorption,[29] based on a large amount of top-down experimental measurements of protein adsorption/desorption. These previous experiments have shown that protein adsorption displays different kinetic regions. Typically for fouling surfaces, the initial adsorption can be spontaneous and generally goes beyond the experimental detection sensibility.[9,10] Prolonged kinetics is observed afterwards leading to a multilayer adsorption build-up.[9]

As an extension of our previous simulation and experimental studies of protein adsorption,[9,11,14] protein docking,[31] and the associated electron transfer,[6,31] we perform here bottom-up atomistic multiscale simulations. Specifically, full-atom MD simulations, free energy computations, and

Langevin Dynamics (LD) simulations are used to study lysozyme adsorption on Au(111) surfaces in a static fluidic aqueous environment in the time scale of microseconds complementing experimental studies. Lysozyme initial conformation was estimated by using free energy calculations performed in a previous study[2] by using a combination of atomistic MD simulations and Molecular Mechanics-Poisson Boltzmann Surface Area (MM-PBSA). In this work, we extend the trajectory up to 100 ns and focus on the estimation of the potential mean force between the protein and the gold surface including polarization effects. Full-atom MD simulations were performed in the NVT ensemble at 298.15 K by using the Gromacs software (version 4.6.5),[32] CHARMM36 force field,[33] GolP-CHARMM polarizable gold surface model,[7] and TIP3P water model in a rectangular box ($8.07 \times 7.99 \times 9.00\,\text{nm}^3$) as shown in Figure S1 in the supplementary material. A net charge of +8e was assigned to the lysozyme crystal structure 1AKI obtained from the Protein Data Bank. The system was neutralized with Cl^- ions. In order to mimic the physiological salt concentration of 150 mM, 39 additional pairs of Na^+ and Cl^- ions were added to the simulation box. Two-dimensional periodic boundary conditions were applied to the system on the *X-Y* plane parallel to the surface. The *Z*-axis is normal to the metallic surface. Simulation of a single-protein adsorption was first performed via a MD simulation for 20 ns at 298.15 K. More details about MD simulations are included in the supplementary material. By using the conformation of 20-ns adsorption, the protein was slowly pulled away from the surface (positive *Z*-direction) using spring with a stiffness constant of 8000 kJ $\text{mol}^{-1}\,\text{nm}^{-2}$ and a pulling rate of 0.00025 nm ps^{-1}. A final displacement of 2.5 nm was achieved at the *Z*-direction. 51 initial configurations were obtained by taking snapshots every 0.05 nm, which were used in umbrella sampling windows.[34,35] MD simulations were performed for each window for 12 ns to collect enough statistics. The weighted histogram analysis method (WHAM)[35,36] was employed to estimate potential of mean force (PMF) between the protein and the polarizable gold surface.

To achieve simulations at larger temporal and spatial scales, Langevin dynamics (LD) simulations were performed using a protein coarse-grained model, which was parameterized with the surface-protein and protein-protein PMF effective interactions

$$m_p \frac{d\bar{v}_p}{dt} = \bar{F}_D + \bar{F}_g + \bar{F}_B + \bar{F}_{P-P} + \bar{F}_{P-S} \qquad (1)$$

in a static environment as shown in Figure S2 in the supplementary material. The drag force ($\bar{F}_D$) is calculated by using the Stokes' law. The net gravity ($\bar{F}_g$) force on a protein immersed in a fluid can be obtained by adding the gravity and buoyancy forces. The random Brownian force ($\bar{F}_B$) acting on the proteins due to the collisions of the solvent particles and ions is estimated from the Einstein theory at a temperature of 298.15 K. Based on the published works of protein association[37,38] and protein surface diffusive behavior[38] with Brownian Dynamics simulations, we performed a systematic investigation of the range of time steps to solve the trajectory. We have chosen a time step of 0.5 ps, which can represent the dynamics of proteins in solution including their interfacial behavior. The protein-protein forces ($\bar{F}_{P-P}$) were taken from the literature[39] including Lennard-Jones interactions and electrostatic interactions through the Debye-Hückel theory for an implicit solvent environment of saline solution with a concentration of 150 mM. The system ($100 \times 30 \times 120\,\text{nm}^3$) consists of 450 coarse-grained proteins (see Figure S2 in the supplementary material). Bulk simulation of 0.1 μs without incorporating the substrate was conducted first before the adsorption. A more detailed discussion about forces and other related properties of the aqueous fluid and the proteins is provided in the supplementary material. COMSOL multiphysics software (Version 5.1, COMSOL Inc. USA) was used to solve the associated ordinary differential equations.

In a previous study,[2] we have shown that the most energetic favorable configuration of the lysozyme to be adsorbed to the metallic surface occurs when the orientation of its dipole moment vector is parallel to the Au(111) surface, and when the distance (*Z*) between the center of the mass (COM) of the protein and the top position of atoms of the gold surface is equal to 1.46 nm. By using the umbrella sampling and the WHAM method, we have estimated the PMF profile as a function of the distance (*Z*) (see Figure 1). The PMF reaches a plateau at the distance $Z \sim 3.5$ nm with the displacement distance of 2.04 nm from the adsorbed configuration. Protein desorption free energy ΔA is around −55 kT calculated by taking the difference of PMF at the final state (i.e., protein in the bulk, $Z = 3.8$ nm) with negligible protein-surface interactions, and the initial state (i.e., protein on the surface, $Z = 1.46$ nm) where the surface is most attractive to the lysozyme molecule. Empirical data fitting was performed to approximate the PMF profile for the following larger scale LD simulations

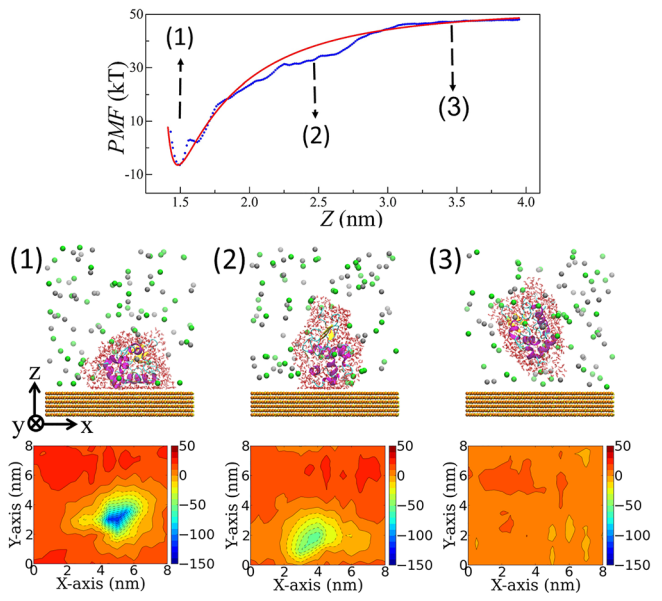

FIG. 1. PMF profile (on the top): data of PMF (blue) and the fitting (red) as a function of the distance *Z*. Three snapshots (at the bottom) include the protein, the first hydration layer of water molecules, and ions, at different gap distances from the surface. The corresponding induced electric field (kJ/mol/e) on the Au (111) surface is also shown in the bottom.

$$\mathrm{PMF} = 81.744\left(\left(\frac{1.368}{Z}\right)^{33} - \left(\frac{1.368}{Z}\right)^{3}\right) + 52.037 \quad (2)$$

where PMF is in the unit of kT and Z is in the unit of nm.

A small transition in the PMF profile is detected at $\Delta Z \sim 0.3$ nm (i.e., $Z \sim 1.75$ nm). Previous studies with neutron scattering experiments[40] and atomistic simulations[14] have shown that in the solution environment, the protein is closely surrounded by a condensed hydration layer of water molecules at the distance of 0.3 nm from the protein's surface, which can lead to an energy barrier for protein adsorption on various substrate neutral-charged surfaces, such as crystallized polyethylene layer,[14] a graphene sheet,[18] and self-assembling monolayer surfaces (SAMs) of azobenzene derivatives.[35] The PMF profile undergoes more transitions due to rotations. To further investigate the effect of protein's hydration on protein adsorption kinetics, another set of LD simulations were conducted by using a smaller time step of 0.01 ps and another PMF profile, which takes into account the sophisticated feature of PMF transition at $Z \sim 1.75$ nm (see Figure S3 and Equation (S1) in the supplementary material). Our results show that protein hydration has a negligible effect overall on the adsorption kinetics of lysozyme (see Figure S4 in the supplementary material).

In order to characterize dynamic electrostatic polarization of the gold surface due to the lysozyme adsorption, the electrostatic potential of the gold surface's image charges is monitored by using an electrostatic potential contour on the X-Y plane, which is divided into 17×17 grids above the top of the substrate surface at 0.3 nm distance from the metallic surface. At each grid point of the position $\bar{r}$, the electric potential $\phi(\bar{r})$ (kJ mol^{-1} e^{-1}) is calculated by summing up the electrostatic interactions over all substrate gold surface atoms N, including the dummy atoms as defined according to the force field parameters

$$\phi(\bar{r}) = 138.935 \sum_{i=1}^{N} \frac{q_i}{|\bar{r} - \overline{r_i}|} \quad (3)$$

with the total atom number N and the position $\overline{r_i}$ of the surface atom i. The electric potential contour shows the overall effect of protein's charge distribution as well as other contributions from the solvent environment, i.e., hydration and ions. Initially, the adsorbed lysozyme is surrounded by water molecules and ions on the Au(111) surface, introducing a pronounced electric polarization response on the gold surface (see the snapshot and $\phi(\bar{r})$ profile for the case 1 in Figure 1). The attractive electrostatic potential is detected in the area of protein's footprint, in contrast to the area outside the footprint, which shows the opposite electrostatic potential (i.e., repulsion potential). When the lysozyme is away from the surface, the surface's induced electric potential becomes smaller (see the snapshot and $\phi(\bar{r})$ profile for the case 2 in Figure 1). It should be noted that in each umbrella sampling window, the protein can freely rotate around its COM, which is constrained by a weak harmonic potential at a certain displacement distance. The protein's rotation and displacement also introduce the re-distribution of water and ions. Eventually when the protein is far away from the surface, the induced electric potential in the gold surface disappears and only shows some small fluctuations (see the snapshot and $\phi(\bar{r})$ profile for case 3 in Figure 1).

We analyzed the changes of the electrostatic (ΔE_{EL}) and LJ (ΔE_{LJ}) interaction energies of the whole Au surface with the protein, water, and ions, respectively, by averaging the last 2-ns trajectory in each umbrella sampling window and by referring to the state of the protein in the bulk (see Figure S5 in the supplementary material). Upon lysozyme desorption, the ΔE_{LJ} for protein-surface interactions is ~ -236.9 kT and the water-surface interaction change is about 172.6 kT. The ΔE_{EL} for protein-surface interactions is around -246.3 kT, and for the water-surface interaction, ΔE_{EL} is around 44.5 kT. However, ions have negligible interactions with the metallic surface ($\Delta E_{LJ} \sim -1.1$ kT and $\Delta E_{EL} \sim -34.6$ kT) at the low ion concentration of 0.15 M. Both proteins and hydration water at the protein-surface interface have dominant interactions with the surface, whereas ions have negligible interactions with the surface. Therefore, it can be concluded that polarization effects on the gold surface are produced mainly by the electrostatic interaction between the metallic surface and the protein at short separation distances.

LD simulations were performed to investigate the multiple-protein adsorption behavior. By monitoring the secondary structures of the adsorbed lysozyme for 100 ns with full-atom MD simulation, no observable structural rearrangements were detected. Therefore, in order to save computational resources, protein molecules are modeled as coarse-grained spheres interacting effectively via their PMF. The bulk space above the gold surface is divided into different layers with the gap distance of 3.0 nm. Figure 2 shows the adsorption kinetics of different layers. The initial protein bulk solution concentration is around 28.6 mg/ml, which is equal to the surface concentration, 0.00858 μg/cm^2 by converting the bulk concentration with the layer gap distance. After 30-μs adsorption, the bulk concentration decays to 14.3 mg/ml (i.e., the surface concentration of 0.00429 μg/cm^2) (see Figure 2). Adsorption of the first layer adjacent to the gold surface increases dramatically, reaching saturation at $\sim$18 μs. However, the second-layer adsorption is much weaker and slower. Another distinct difference is the onset of adsorption. An initial rapid depletion (i.e., $t < 0.5$ μs) of the second-layer occurs, due to the mass transfer to the bottom layer (see the inset of Figure 2). The 2nd-layer adsorption starts, after the

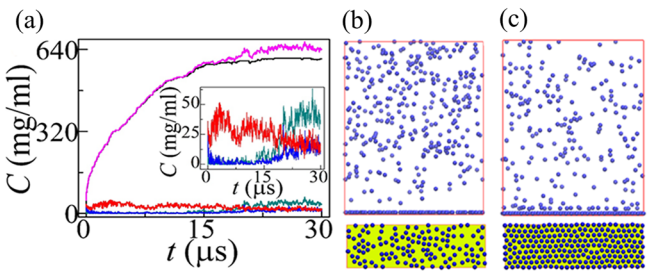

FIG. 2. (a) Protein adsorption in a static fluidic environment simulated with LD simulation: the adsorption kinetics profiles (the 1st layer colored black, the 2nd layer colored cyan, the 3rd layer colored blue, the bulk in red, and the total of 1st and 2nd layers colored pink). The inset shows the concentration profile for the 2nd, 3rd and the bulk with the first 30 μs. Snapshots at different times ((b): 5 μs; (c): 20 μs): the side view and the top view of protein adsorption. (For the top view, only the first layer adsorption is shown for the sake of clarity.)

first adsorption layer is almost fully developed at ~18 μs. The difference of adsorption kinetics between the 1st-layer and the 2nd-layer is attributed to the strong protein-surface interactions (~−55 kT) and the weak protein-protein interactions.[39] Protein molecules in the first layer are tightly bound onto the gold substrate, whereas proteins at the 2nd layer which are mostly under the effects of first layer proteins are loosely packed, which is evidenced by the slower adsorption kinetics of the 2nd layer (Figure 2(a)) and configurations (see Figures 2(b) and S6 (supplementary material)). The 3rd-layer also undergoes initial depletion and the re-filling takes place at the same time as the adsorption of the 2nd-layer reaching the same concentration as that in the bulk in 30 μs. Including the adsorption in the 2nd layer, the total surface concentration is 646.7 mg/ml (i.e., the surface concentration of 0.194 μg/cm^2) after 30 μs. The first-layer saturation concentration is around 506.7 mg/ml (i.e., surface concentration of 0.179 μg/cm^2) as the bulk concentration reaches 14.3 mg/ml. The protein concentration profile, as shown in Figure 3(a) along the direction of the surface normal, also suggests that the protein surface concentration decays to the bulk value (0.00429 μg/cm^2) for $Z > 6.0$ nm, which again indicates the adsorption around 2 layers in 30 μs. To validate the accuracy of our simulation, another simulation was conducted at lower bulk concentration. The repeated simulations show that when the final bulk concentration is around 0.13 mg/ml, the final equilibrium surface concentration of the monolayer is about 0.116 μg/cm^2, matching experimental measurements, 0.098–0.119 μg/cm^2 at the bulk concentration of 0.1 mg/ml in the literature.[27,41]

Weak protein surface aggregation is observed during the course of adsorption before reaching the full coverage of the surface, i.e., the monolayer adsorption (see Figure 2(b) and see Figure S6 in the supplementary material). Protein molecules aggregate and form small clusters randomly distributed on the surface, at the initial adsorption. It is noteworthy that our previous study with computational fluid dynamics simulations[2] revealed that protein adsorption can exhibit an S-shape with an increase in the adsorption rate at the beginning, followed by a decreasing adsorption rate due to the coupling of convection, diffusion, and surface fouling reactions during mass transfer at the transition-state. However, our LD simulation shows that in a static fluidic environment, the adsorption kinetics for lysozyme on the Au(111) surface displays a convex shape with a rapid initial increase followed by prolonged adsorption (see Figure 2).

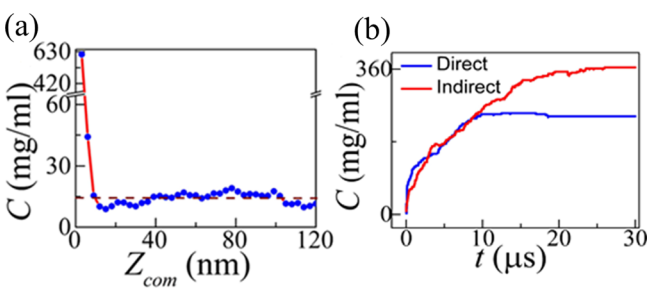

FIG. 3. (a) Concentration profile (C) as a function of the distance (Z) to the surface after 30-μs of LD simulation. The bulk concentration is indicated with a brown dashed line; (b) direct and indirect adsorption kinetics.

By tracking molecular trajectories, protein's most frequent interfacial motions were analyzed. For the adsorption of the first layer, two types of motions can be identified: the direct adsorption from the bulk onto the surface and the indirect adsorption, which includes protein bumping on the surface and the rollover of the previously adsorbed proteins. To differentiate the direct and indirect adsorption, we adopt the criteria of residence time inside the 2nd layer: $\tau < 19$ ns for direct adsorption and $\tau > 19$ ns for indirect adsorption. The histogram of protein's residence time also shows that most proteins' residence time in the 2nd layer is around 19 ns (see Figure S7 in the supplementary material), which is close to the time scale (18 ns) for diffusion across such a distance of 3.0 nm. The direct and indirect adsorption kinetics is compared in Figure 3(b). Around 40% of the proteins are directly adsorbed onto the surface, dominating the initial stage covering 33% of the total adsorption time. In contrast, the remaining 60% proteins are adsorbed onto the surface indirectly, mainly in the last stage (67% of the total time).

In summary, in this work, we have performed bottom-up multiscale simulations to reveal the adsorption and interfacial behavior of lysozyme and a Au(111) surface including polarization effects. Our simulations precisely predict the adsorption amount, and we interpret the metallic surface polarization and heterogeneous adsorption kinetics for different layers by correlating the short and long range molecular interactions. Our fundamental research is paving the road for future research in biosensor development, e.g., the method of TIMEs to detect protein-ligand interactions via polarization signals induced in metallic electrodes.

See supplementary material for details on the MD and LD simulations, adsorption kinetic profile, interaction energies, protein adsorption process, and protein residence time.

This research was supported by the NSF/XSEDE program and Texas Advanced Computing Center.

[1]T. T. Zhang, T. H. Ku, Y. Y. Han, R. Subramanian, I. A. Niaz, H. Luo, D. Chang, J. J. Huang, and Y. H. Lo, Sci. Rep. **6**, 35570 (2016).
[2]T. T. Zhang, T. Wei, Y. Y. Han, H. Ma, M. Samieegohar, P. W. Chen, I. Lian, and Y. H. Lo, ACS Cent. Sci. **2**(11), 834 (2016).
[3]P. B. Messersmith, Science **319**(5871), 1767 (2008).
[4]A. J. Keefe and S. Y. Jiang, Nat. Chem. **4**(1), 59 (2012).
[5]J. Bellas, Sci. Total Environ. **367**(2–3), 573 (2006).
[6]T. Wei, H. Ma, and A. Nakano, J. Phys. Chem. Lett. **7**(5), 929 (2016).
[7]L. B. Wright, P. M. Rodger, S. Corni, and T. R. Walsh, J. Chem. Theory Comput. **9**(3), 1616 (2013).
[8]Z. E. Hughes, L. B. Wright, and T. R. Walsh, Langmuir **29**(43), 13217 (2013).
[9]T. Wei, S. Kaewtathip, and K. Shing, J. Phys. Chem. C **113**(6), 2053 (2009).
[10]G. Cheng, G. Z. Li, H. Xue, S. F. Chen, J. D. Bryers, and S. Y. Jiang, Biomaterials **30**(28), 5234 (2009).
[11]C. M. Nakano, H. Ma, and T. Wei, Appl. Phys. Lett. **106**(15), 153701 (2015).
[12]S. F. Chen, Z. Q. Cao, and S. Y. Jiang, Biomaterials **30**(29), 5892 (2009).
[13]J. Satulovsky, M. A. Carignano, and I. Szleifer, Proc. Natl. Acad. Sci. U. S. A. **97**(16), 9037 (2000).
[14]T. Wei, M. A. Carignano, and I. Szleifer, Langmuir **27**(19), 12074 (2011).
[15]K. Rechendorff, M. B. Hovgaard, M. Foss, V. P. Zhdanov, and F. Besenbacher, Langmuir **22**(26), 10885 (2006).
[16]Y. Arima and H. Iwata, Biomaterials **28**(20), 3074 (2007).
[17]T. Wei, M. A. Carignano, and I. Szleifer, J. Phys. Chem. B **116**(34), 10189 (2012).
[18]F. C. D. A. Lima, A. Calzolari, M. J. Caldas, R. M. Iost, F. N. Crespilho, and H. M. Petrilli, J. Phys. Chem. C **118**(40), 23111 (2014).

[19]D. Golze, M. Iannuzzi, M. T. Nguyen, D. Passerone, and J. Hutter, J. Chem. Theory Comput. **9**(11), 5086 (2013).
[20]Z. E. Hughes, S. M. Tomasio, and T. R. Walsh, Nanoscale **6**(10), 5438 (2014).
[21]H. Heinz, K. C. Jha, J. Luettmer-Strathmann, B. L. Farmer, and R. R. Naik, J. R. Soc. Interface **8**(55), 220 (2011).
[22]M. Ozboyaci, D. B. Kokh, S. Corni, and R. C. Wade, Q. Rev. Biophys. **49**, e4 (2016).
[23]M. Rabe, D. Verdes, and S. Seeger, Adv. Colloid Interface Sci. **162**(1–2), 87 (2011).
[24]J. Talbot, G. Tarjus, P. R. Van Tassel, and P. Viot, Colloids Surf., A **165**(1–3), 287 (2000).
[25]G. J. Szollosi, I. Derenyi, and J. Voros, Physica A **343**, 359 (2004).
[26]S. M. Daly, T. M. Przybycien, and R. D. Tilton, Langmuir **19**(9), 3848 (2003).
[27]D. Z. Shen, M. H. Huang, L. M. Chow, and M. S. Yang, Sens. Actuators, B **77**(3), 664 (2001).
[28]L. K. Koopal and M. J. Avena, Colloids Surf., A **192**(1–3), 93 (2001).
[29]A. P. Minton, Biophys. J. **80**(4), 1641 (2001).
[30]M. Rabe, D. Verdes, J. Zimmermann, and S. Seeger, J. Phys. Chem. B **112**(44), 13971 (2008).
[31]C. M. Nakano, H. S. Byun, H. Ma, T. Wei, and M. Y. El-Naggar, Comput. Phys. Commun. **193**, 1 (2015).
[32]B. Hess, C. Kutzner, D. van der Spoel, and E. Lindahl, J. Chem. Theory Comput. **4**(3), 435 (2008).
[33]A. D. MacKerell, D. Bashford, M. Bellott, R. L. Dunbrack, J. D. Evanseck, M. J. Field, S. Fischer, J. Gao, H. Guo, S. Ha, D. Joseph-McCarthy, L. Kuchnir, K. Kuczera, F. T. K. Lau, C. Mattos, S. Michnick, T. Ngo, D. T. Nguyen, B. Prodhom, W. E. Reiher, B. Roux, M. Schlenkrich, J. C. Smith, R. Stote, J. Straub, M. Watanabe, J. Wiorkiewicz-Kuczera, D. Yin, and M. Karplus, J. Phys. Chem. B **102**(18), 3586 (1998); R. B. Best, X. Zhu, J. Shim, P. E. M. Lopes, J. Mittal, M. Feig, and A. D. MacKerell, J. Chem. Theory Comput. **8**(9), 3257 (2012).
[34]G. M. Torrie and J. P. Valleau, J. Comput. Phys. **23**(2), 187 (1977).
[35]T. Wei, M. S. J. Sajib, M. Samieegohar, H. Ma, and K. Shine, Langmuir **31**(50), 13543 (2015).
[36]S. Kumar, J. M. Rosenberg, D. Bouzida, R. H. Swendsen, and P. A. Kollman, J. Comput. Chem. **13**(8), 1011 (1992).
[37]G. Wieczorek and P. Zielenkiewicz, Biophys. J. **95**(11), 5030 (2008).
[38]C. Gorba, T. Geyer, and V. Helms, J. Chem. Phys. **121**(1), 457 (2004).
[39]M. C. Abramo, C. Caccamo, D. Costa, G. Pellicane, and R. Ruberto, J. Phys. Chem. B **114**(28), 9109 (2010).
[40]F. Merzel and J. C. Smith, Proc. Natl. Acad. Sci. U. S. A. **99**(8), 5378 (2002).
[41]H. R. Luckarift, S. Balasubramanian, S. Paliwal, G. R. Johnson, and A. L. Simonian, Colloids Surf., B **58**(1), 28 (2007).